Supporting Information

Drug Binding Disrupts Chiral Water Structures in the DNA First Hydration Shell

Ty Santiago[1a], Daniel Konstantinovsky[1,2§a], Matthew Tremblay[1,3a], Ethan A. Perets[1#]*, Sharon Hammes-Schiffer[1,3]*, Elsa C. Y. Yan[1]*

[1]Department of Chemistry, Yale University, New Haven, CT 06520, USA

[2]Department of Molecular Biophysics and Biochemistry, Yale University, New Haven, CT 06520, USA

[3]Department of Chemistry, Princeton University, Princeton, New Jersey 08544, USA

[§]Current Address: Department of Chemistry, Columbia University, New York, New York 10027, USA

[#]Current Address: Department of Molecular Biology, University of Texas Southwestern Medical Center, Dallas, TX 75390, USA

[a]Equal Contribution

*Corresponding Authors; email: ethan.perets@utsouthwestern.edu, shs566@princeton.edu, elsa.yan@yale.edu

Experimental Methods

Sample Preparation

Single-stranded $(dA)_{12}$ and $(dT)_{12}$ DNA oligomers were purchased from the Keck Oligonucleotide Synthesis Resource at Yale University, which were HPLC purified and used without further purification. Solutions of $(dA)_{12}\cdot(dT)_{12}$ dsDNA were prepared in water (Millipore Synergy UV-R system, 18.2 MΩ) at a concentration of 200 μM by annealing single-stranded $(dA)_{12}$ and $(dT)_{12}$ at 80 ºC for 10 minutes and allowing the solution to cool down at room temperature in a water bath. DNA solutions were then stored at 4 ºC.

Netropsin dihydrochloride (Enzo Life Sciences, ALX-380-088-M005) was procured as a lyophilized powder and prepared as a 1 mM solution in H_2O (Millipore Synergy UV-R system, 18.2 MΩ). Netropsin solution was mixed with the 200 μM $(dA)_{12}\cdot(dT)_{12}$ dsDNA and then diluted to give a final concentration of dsDNA at 100 μM and netropsin at 0 μM, 100 μM, 150 μM, or 200 μM. The mixtures were incubated at room temperature for at least one hour and were subsequently stored at 4ºC. An aliquot of 10 μL of the DNA-netropsin solutions was applied to the surface of quartz and subsequently dried in a desiccator to yield a hydrated film. We recorded the phase-resolved chiral SFG spectra of the hydrated DNA films on the surface of a right-handed z-cut α-quartz crystal (Conex Systems Technology Inc., San Jose, CA). Prior to sample preparation the quartz was cleaned by rinsing with H_2O, dried with nitrogen, and plasma-cleaned (Harrick Plasma; PDC-32G) on "low" for 15 min.

Acquisition of phase-resolved vibrational SFG spectra

A home-built broad-bandwidth SFG spectrometer[1, 2] was used to acquire phase-resolved chiral SFG spectra of the hydrated DNA-netropsin films.[3] The *psp*-polarization (*p*-polarized sum frequency, *s*-polarized visible, *p*-polarized infrared) was used to acquire the chiral SFG spectra. Spectral frequencies were calibrated using a polystyrene reference (Buck Scientific), and cosmic rays were manually removed.[1] The spectra were recorded with the $+y$ and $-y$ axes of the quartz oriented parallel to the incident plane.[4-6] At each orientation, 10 spectra were recorded for 2 minutes. The averaged spectra were normalized to the spectrum of a clean quartz substrate. The difference between the $+y$ (I_{+y}) and $-y$ (I_{-y}) spectra yields the imaginary component of the second-order susceptibility, $Im[\chi^{(2)}]$:

$$Im[\chi^{(2)}] = \frac{(I_{+y} - I_{-y})}{4} \qquad (1)$$

Analyses of experimental chiral SFG spectra

Chiral SFG signals of water contain contributions from the symmetric and asymmetric stretching modes of water in equal magnitudes but with opposite phase.[7] These two modes generate non-zero chiral SFG signal due to intramolecular coupling, yielding a unique lineshape of a doublet in opposite phases. Hence, we used the following function containing two terms to fit the chiral SFG spectra of the netropsin-DNA samples containing NH stretches of dsDNA and netropsin, and OH stretches of water:

where A_q, Γ_q, and ω_q are the amplitude, width, and vibrational frequency of the q^{th} vibrational modes other than water OH stretches; A_n and Γ_n and are the amplitude and widths of the n^{th} pair of water OH symmetric and asymmetric stretches; and $\Delta\nu_n$ and ω_n are the frequency difference and average of the n^{th} symmetric and asymmetric water OH stretches, respectively. The first term represents the independent Lorentzian

$$f(\omega_{IR}) = Im\left[\sum_q \frac{A_q}{\omega_{IR} - \omega_q - i\Gamma_q} + \sum_n \frac{A_n}{\omega_{IR} - \left(\omega_n + \frac{1}{2}\Delta\nu_n\right) - i\Gamma_n} - \frac{A_n}{\omega_{IR} - \left(\omega_n - \frac{1}{2}\Delta\nu_n\right) - i\Gamma_n}\right] \quad (2)$$

peaks used to fit vibrational bands that are not associated with the chiral SFG response of water OH stretches, such as NH stretches of dsDNA and netropsin in our studies. The second term is the coupled symmetric and asymmetric stretches of water, which takes the form of a pair of positive and negative peaks of the same magnitude and width, separated from their average frequency (ω_n) by $\pm\frac{1}{2}\Delta\nu_n$.

Using Equation 2, we globally fit the chiral SFG spectra at various netropsin:dsDNA molar ratios of 0:1, 1:1, 1.5:1, and 2:1 (Figure 2). In our previous study,[2] we used Equation 2 to fit the spectrum of $(dA)_{12}\cdot(dT)_{12}$ dsDNA obtained in H_2O guided by isotopic studies using $H_2{}^{18}O$. From this previous study, we obtained the numerical values of the center peak positions (ω_n), peak widths (Γ_n), and frequency differences ($\Delta\nu_n$) for the two pairs of OH stretching bands of water, and the NH stretching frequencies (ω_q) and peak widths (Γ_q) from the $(dA)_{12}\cdot(dT)_{12}$ dsDNA spectrum acquired in H_2O in the absence of netropsin. Here, we kept the same numerical values in our global fitting of the four spectra presented in Figure 2 but let the amplitudes (A_q and A_n) of the corresponding OH stretching bands of water and NH stretching bands of the dsDNA float freely. Additionally, based on residual analysis (orange, Figure 2), we incorporated an extra Lorentzian peak in fitting the two spectra obtained at higher netropsin molar ratios (1.5:1 and 2:1). We set the position, width, and amplitude of this extra peak as free parameters in addition to the OH and NH amplitudes (A_q and A_n) in our global fitting of the four spectra shown in Figure 2 (see table S1for fitting results).

Spectral Fitting Parameters

Parameter	[Netropsin]:[dsDNA]				Assignment
	0	1:1	1.5:1	2:1	
A_1	-31.08 ± 4.71	-23.36 ± 4.60	-9.89 ± 5.02	-4.03e-15 ± 6.69	Water OH
v_1	3503.20	3503.20	3503.20	3503.20	
Δv_1	149.98	149.98	149.98	149.98	
Γ_1	80.83	80.83	80.83	80.83	
A_2	78.21 ± 9.50	51.18 ± 6.15	51.47 ± 7.33	67.92 ± 8.04	DNA NH
v_2	3399.70 ± 3.72	3399.70 ± 3.72	3399.70 ± 3.72	3399.70 ± 3.72	
Γ_2	48.26 ± 4.22	48.26 ± 4.22	48.26 ± 4.22	49.33 ± 4.22	
A_3	-16.64 ± 7.70	-5.18 ± 3.98	-8.19 ± 4.80	-6.13 ± 4.75	DNA NH
v_3	3347.10 ± 3.49	3347.10 ± 3.49	3347.10 ± 3.49	3347.10 ± 3.49	
Γ_3	21.07 ± 7.54	21.07 ± 7.54	21.07 ± 7.54	21.07 ± 7.54	
A_4	159.98 ± 15.20	97.68 ± 12.10	67.61 ± 15.00	49.33 ± 11.70	Water OH
v_4	3222.50	3222.50	3222.50	3222.50	
Δv_4	79.22	79.22	79.22	79.22	
Γ_4	95.06	95.06	95.06	95.06	
A_5	-111.65 ± 3.80	-78.47 ± 3.15	-96.45 ± 3.51	-63.42 ± 3.07	DNA NH
v_5	3208.60 ± 1.25	3208.60 ± 1.25	3208.60 ± 1.25	3208.60 ± 1.25	
Γ_5	38.80 ± 1.46	38.80 ± 1.46	38.80 ± 1.46	38.80 ± 1.46	
A_6	0.00	0.00	10.17 ± 2.75	25.07 ± 2.68	Netropsin NH
v_6	3510.20 ± 4.17	3510.20 ± 4.17	3510.20 ± 4.17	3510.20 ± 4.17	
Γ_6	33.77 ± 7.91	33.77 ± 7.91	33.77 ± 7.91	33.77 ± 7.91	

Table S1. Global fitting parameters for chiral SFG spectra of $(dA)_{12}\cdot(dT)_{12}$ dsDNA with molar netropsin:dsDNA ratios of 0:1, 1:1, 1.5:1, and 2:1 (Figure 2) using Equation 2. The first column shows the parameters for the n^{th} vibrational band. All amplitude (A_n) values are in arbitrary units. The peak center frequency (ω_n), peak half width at half maximum (Γ_n), and differences in vibrational frequency (Δv_n) are in wavenumber (cm^{-1}). The Δv_n parameter denotes the frequency difference between two peaks in one pair of water OH stretches.

Computational Methods

Molecular dynamics calculations

A $(dA)_{12}\cdot(dT)_{12}$ dsDNA model was constructed using the AMBER Nucleic Acid Builder.[8] To model netropsin, the RESP procedure was used to assign AMBER charge parameters, and other parameters were selected from GAFF. The DNA structure was aligned to a crystal structure of DNA with one (PDB: 6BNA)[9] or two (PDB: 358D)[10] netropsin molecules using VMD.[11] All three systems (zero, one, and two netropsin molecules) were solvated with TIP4P-Ew water[12] and neutralized with sodium ions using AMBER's *tleap* program. Netropsin-containing systems were energy-minimized with restraints on the DNA (force constants of 500 kcal mol^{-1} $Å^{-2}$) to allow the netropsin to relax to a more favorable conformation. Following this minimization, MD simulations were carried out as described in our previous work on chiral SFG of DNA.[2] Briefly, the systems were minimized in phases with gradually loosening restraints on the DNA and netropsin until all restraints were released. The systems were then gradually heated in the NPT ensemble from 0 K to 300 K. The systems were finally equilibrated in the NPT ensemble for 5 ns and then in the NVT ensemble for 5 ps. To obtain trajectories, the system was propagated for 100 ns in the NVT ensemble, with coordinates saved every 100 fs.

Calculations of water spectra

SFG spectra of water were calculated from MD simulations using the electrostatic mapping approach developed by the Skinner lab.[13-17] The inhomogeneous limit approximation was applied to the time-correlation function. Within each frame, the system was rotated such that the sixth thymine's N3-H3 bond (Scheme 1b) was aligned with the *y*-axis, with the positive direction pointing toward the hydrogen atom. The *x*-axis was chosen to point toward the thymine O2 while remaining orthogonal to the *y*-axis. Consequently, the z-axis pointed along the helical axis of the DNA, perpendicular to the base pair. Since the experimental orientation of dsDNA relative to the interface is unknown, the absolute phase of the calculated water spectra cannot be directly compared to that measured experimentally. However, the relative phases and amplitudes can be compared to experimental data. To reproduce the absolute phases observed experimentally, all calculated water spectra were multiplied by -1. For calculations involving a subset of waters, the SFG response is only a direct result of those particular waters, but all other atoms in the system also contribute to the electric field felt by each OH group within that subset.

Selection of Water Molecule Subsets

For full details of selections of the water subsets associated with the major groove, minor groove, and backbone, see our previous work on chiral SFG of dsDNA.[2] Briefly, the waters constituting the first hydration shell of dsDNA were selected by Voronoi tessellation.[18] Voronoi tessellation divides space into regions that consist of all points that are closer to a given atom than they are to any other atom. Two atoms are defined as neighbors if the Voronoi tesserae that surround them share a face, and two molecules are defined as neighbors if any of their constituent atoms are neighbors. The first hydration shell consists of all water molecules that are neighbors of any part of the DNA, and the first hydration shell can then be divided into further subsets. Major groove water molecules were chosen as those that were closer to any atom of the major groove than to any other group in the DNA. Minor groove water molecules were chosen as those within 3.5 Å of H2 on any adenine residue. Backbone water molecules were chosen by a distance criterion analogous to that of the major groove followed by removal of water molecules near those of the minor groove to avoid contamination from the strong signal of the minor groove. For the subset of water molecules forming a strong hydrogen bond with the thymine C2=O carbonyl in the minor groove (Scheme 1b), the minor groove water selection was further filtered to select water molecules with an H_{water}-$O_{carbonyl}$ distance of 1.6 Å or less and an O_{water}-H_{water}-$O_{carbonyl}$ angle of 135° or greater. Atom selections were performed using MDAnalysis[19, 20] and in-house Python code. Voronoi tessellation was performed using the Freud library[21] to access voro++.[22]

Simulated and Experimental Vibrational Spectra of Netropsin

The peak at 3510 cm^{-1} in the experimental spectra obtained at the netropsin:dsDNA molar ratios of 1.5:1 and 2:1 (Figure 2) is proposed to arise from the NH stretches of netropsin upon binding to the minor groove of $(dA)_{12}\cdot(dT)_{12}$ dsDNA. To evaluate this possibility, we calculated the vibrational spectra of netropsin and acquired experimental infrared spectra of lyophilized netropsin powder in the frequency range from 3000 cm^{-1} to 3800 cm^{-1} (Figure S1). To generate the simulated spectra, density functional theory (DFT) calculations of netropsin were performed with Gaussian 16.[1] A netropsin structure was extracted from the equilibrated 1:1 dsDNA-netropsin complex. This starting geometry was optimized twice independently. One optimization used the conductor-like polarizable continuum model[2] (CPCM) to implicitly solvate with water (Figure S1a), and the other was performed in the gas phase (Figure S1b). This was done to examine the effect of solvation on the vibrational modes of netropsin. In the dsDNA minor groove, the dielectric constant is ~20 D, which is between that of water and vacuum.[3] Both geometry optimizations were carried out with the ωB97XD functional[4] and the 6-311+G(d,p) basis set.[5] Following optimization, a harmonic normal mode analysis was carried out at the same level of theory to predict the infrared and Raman spectra of each of the two optimized netropsin geometries. These spectra can serve as a crude estimate for modes that may be detectable via chiral SFG, as only modes that are both infrared-active and Raman-active are vibrational SFG-active.[6] In the simulated spectra, calculated frequencies were scaled by 0.95 (standard for the ωB97XD functional)[7] for comparison to experiment, and the peak widths were set to a value of 5 cm^{-1} for depiction. Figures S1a and S1b shows the simulated spectra using CPCM and gas phase, respectively, which are compared with the experimental infrared spectrum (Figure S1c). The combined computational and experimental spectra reveal a cluster of vibrational bands above 3500 cm^{-1} due to amidine stretches in the end group of the netropsin, supporting our assignment of the 3510-cm^{-1} vibrational band in the experimental chiral SFG spectra (Figure 2) to netropsin binding to $(dA)_{12}\cdot(dT)_{12}$ dsDNA.

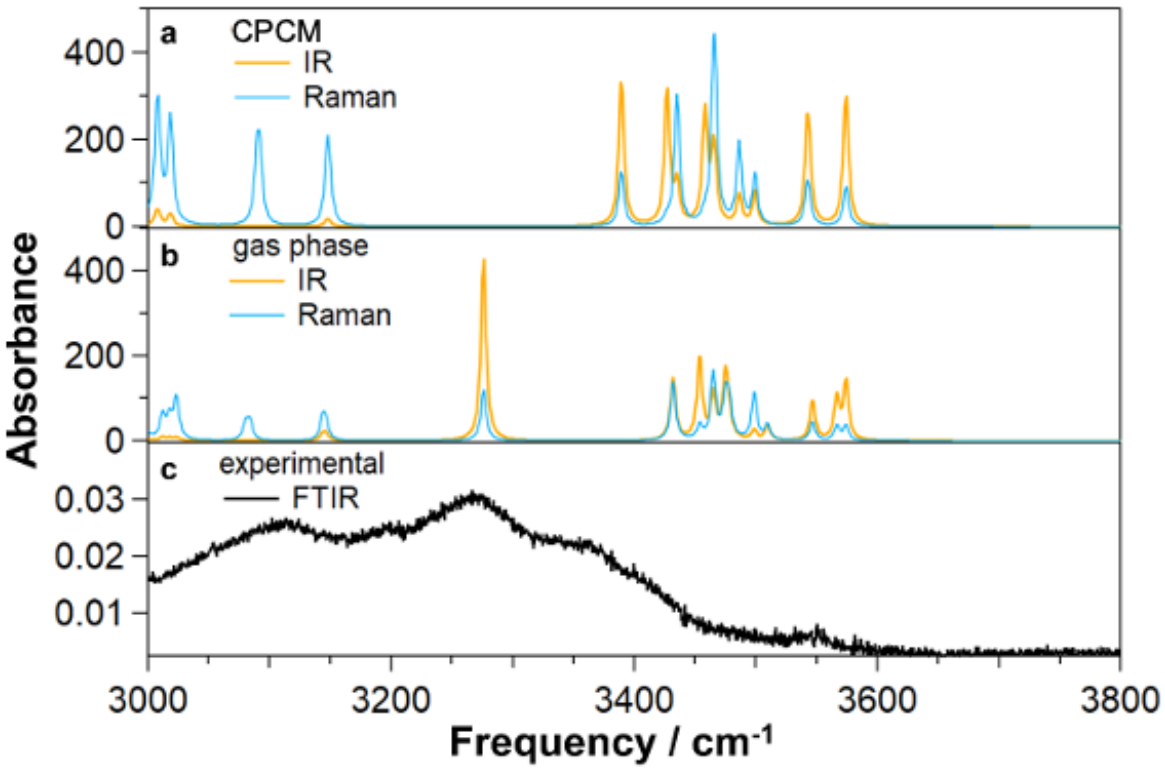

Figure S1. Simulated and experimental vibrational spectra of netropsin from 3000 cm^{-1} to 3800 cm^{-1}. (a) Simulated infrared (orange) and Raman (blue) spectra of netropsin in implicit water. (b) Simulated infrared (orange) and Raman (blue) spectra in the gas phase. (c) Experimental infrared spectrum of lyophilized netropsin powder. For simulated DFT spectra, frequencies were scaled by 0.95.[7] Spectra were calculated at the ωB97XD/6-311+G(d,p)[4,5] level of theory using Gaussian 16.[1] Simulated spectra were represented with a half width at half maximum of 5 cm^{-1}.

Analysis of Simulated Chiral SFG Spectra of Strongly H-Bonded Water in the Minor Groove

The experimental spectra in Figure 2 show two pairs of water OH stretches centered at 3503 cm^{-1} and 3223 cm^{-1}, implying that there are at least two distinctly different H-bonding environments for water molecules within the minor groove. Our simulated spectra in Figure 1a predict only a single pair of peaks from the water OH stretches centered at 3400 cm^{-1} (Figure S2b). In previous studies we have noted that Skinner's OH map underestimates the impact of hydrogen bonding to carbonyl groups of proteins because the map was parameterized with bulk water.[3] To determine if the experimental water peak pair centered at 3223 cm^{-1} is generated by water molecules strongly H-bonded to the carbonyl within the minor groove, we selected a specific subset of minor groove water molecules that donate a hydrogen bond to the thymine C2=O group (see Scheme 1b) with an H_{water}-$O_{carbonyl}$ distance of 1.6 Å or less and an O_{water}-H_{water}-$O_{carbonyl}$ angle of 135° or greater. Figure S3a shows simulated chiral SFG spectra (gray curves), the fitting curves (black curves), and the residuals of the fitting (orange curves) for the $(dA)_{12}\cdot(dT)_{12}$ dsDNA molecule complexed with 0, 1, and 2 netropsin molecules (from left to right). Figure S3b shows the simulated symmetric (blue curves) and asymmetric (red curves) OH stretch chiral SFG signals. Figure S3c shows two pairs of water OH stretching bands centered at 3097 and 3332 cm^{-1} obtained by fitting the chiral SFG spectra (gray curves) shown in Figure S3a. Compared to the OH stretching frequency of all water molecules in the first hydration shell at 3400 cm^{-1} (Figure S1b), these frequencies of water forming strong H-bonds in the minor groove are significantly red shifted to lower frequencies. These low-frequency bands are under-represented in the simulation using the OH electrostatic map. Hence, although they contribute to the first hydration shell spectrum (Figure S1), their intensities are masked by signals from other water molecules in the first hydration shell.

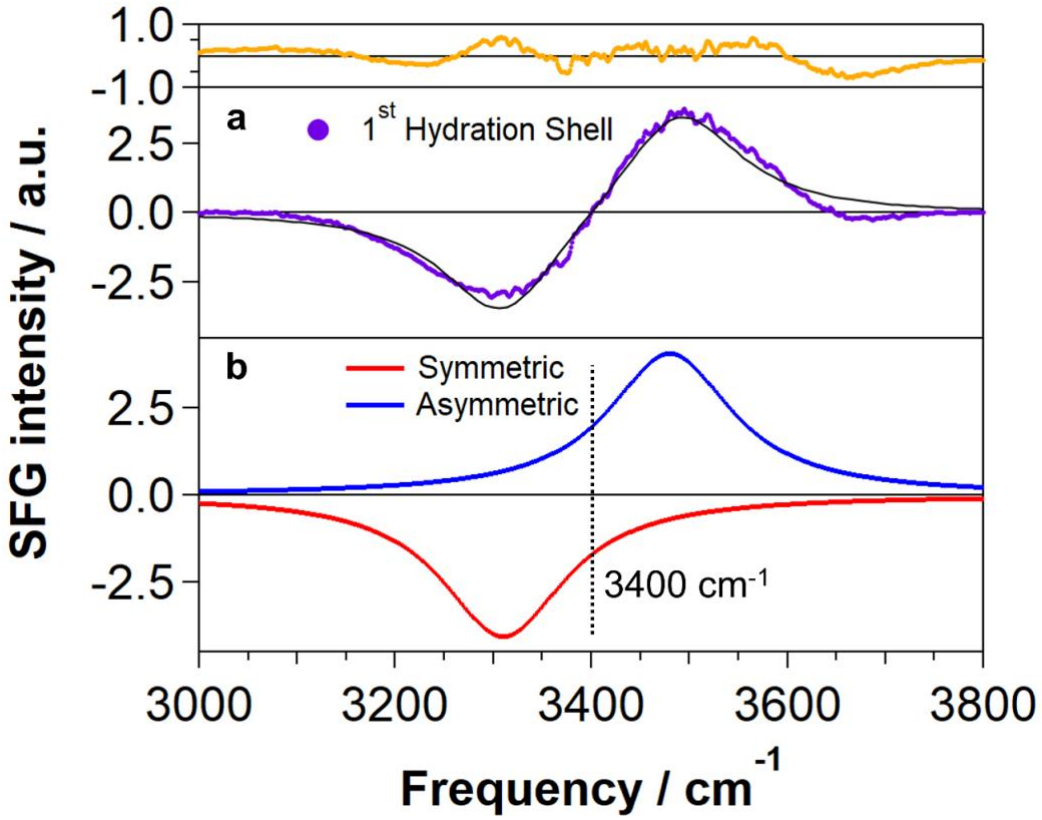

Figure S2. Simulated chiral SFG spectra of OH stretches of water in the first hydration shell of $(dA)_{12}\cdot(dT)_{12}$ dsDNA. (a) Simulated chiral SFG spectra of OH stretching (purple), fitting curve (black), and residual of the fitting (orange). (b) A pair of symmetric (blue) and asymmetric (red) peaks from water OH stretching obtained from the fitting of the simulated spectrum (purple).

dsDNA First Hydration Shell	
Parameter	Value
A_1	-312.58 ± 3.23
v_1	3399.60 ± 3.23
Δv_1	179.48
Γ_1	77.07 ± 0.77

Table S2. Fitting parameters for the computational chiral SFG spectrum shown in Figure S2 for water in the first hydration shell of $(dA)_{12}\cdot(dT)_{12}$ dsDNA.

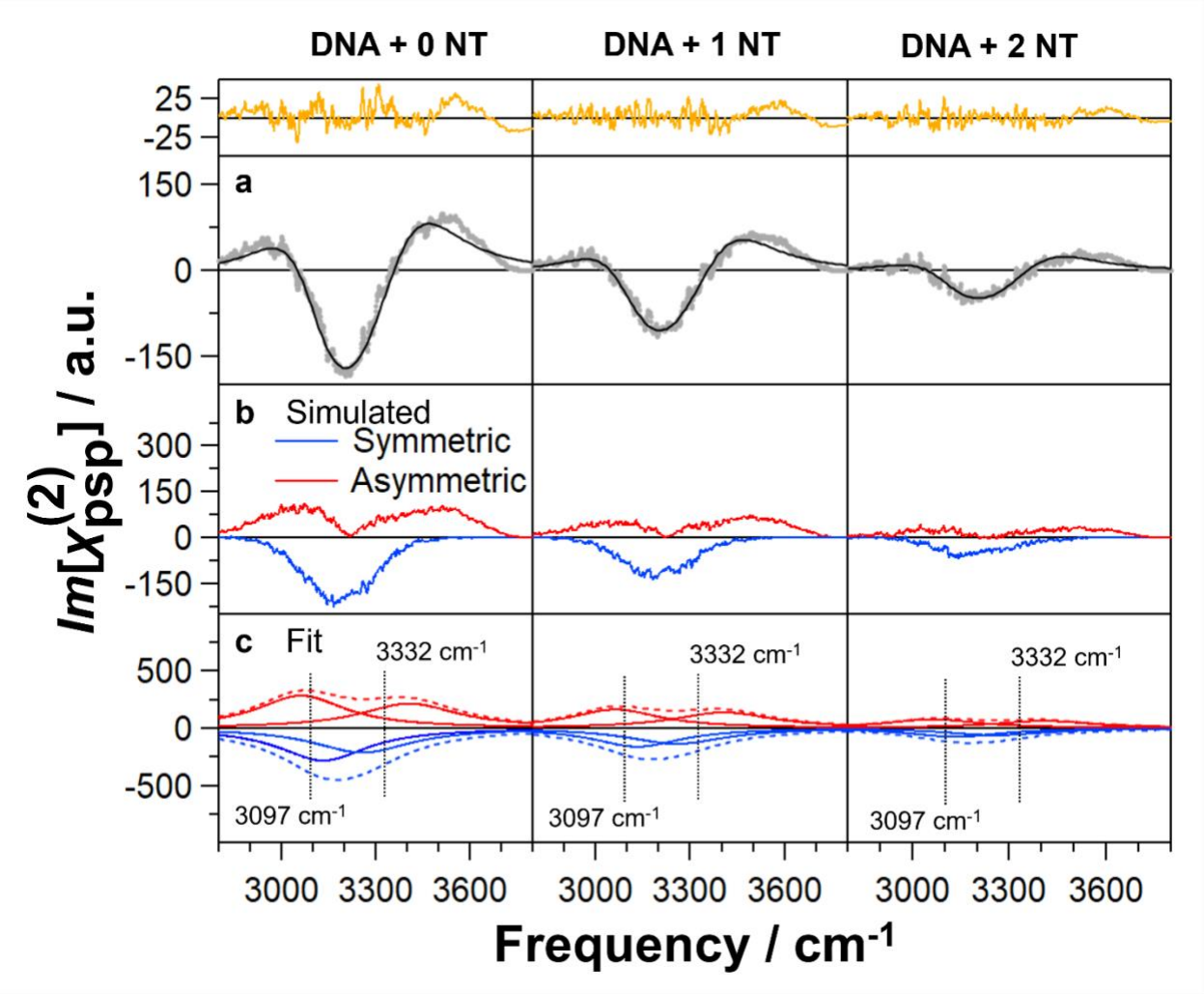

Figure S3. Simulated chiral SFG spectra of OH stretches of water in the minor groove of $(dA)_{12}\cdot(dT)_{12}$ dsDNA that are H-bonded to the C2=O carbonyl of thymine. Columns show data corresponding to dsDNA complexed with 0, 1, and 2 netropsin (NT) molecules. (a) Simulated chiral SFG spectra of OH stretches (gray), with the fitting curve (black) and residual (orange). (b) Simulated symmetric (blue) and asymmetric (red) stretches of the same subset of water H-bonded to the thymine C2=O group. (c) Two pairs of symmetric (blue) and asymmetric (red) component peaks obtained from fitting the simulated spectra (gray) to generate the fitting curves (black). The solid red and blue lines show the individual peaks, and the dashed red and blue lines represent the sum of the symmetric and asymmetric OH stretches. Dotted vertical lines mark the two pairs of water peaks centered at 3097 cm^{-1} and 3332 cm^{-1}. Water molecules were selected with the protocol for the minor groove (see Methods) with an additional restriction that they are donating a hydrogen bond to the C2=O carbonyl of a thymine nucleotide with an H_{water}-$O_{carbonyl}$ distance of 1.6 Å or less and an O_{water}-H_{water}-$O_{carbonyl}$ angle of 135° or greater.

Parameter	dsDNA + 0 NT	dsDNA + 1 NT	dsDNA + 2 NT
A_1	49.09 ± 1.17	28.12 ± 0.75	13.23 ± 0.46
v_1	3097.00 ± 1.12	3097.00 ± 1.12	3097.00 ± 1.12
Δv_1	70.12	70.12	70.12
Γ_1	172.77 ± 1.91	172.77 ± 1.91	172.77 ± 1.91
A_2	-40.09 ± 0.64	-26.29 ± 0.43	-11.97 ± 0.26
v_2	3331.80 ± 0.99	3331.80 ± 0.99	3331.80 ± 0.99
Δv_2	149.16	149.16	149.16
Γ_2	191.16 ± 1.63	191.16 ± 1.63	191.16 ± 1.63

Table S3. Global fitting parameters for simulated chiral SFG spectra shown in Figure S3 for strongly H-bonded water in the minor groove of $(dA)_{12} \cdot (dT)_{12}$ dsDNA complexed with 0, 1, and 2 netropsin (NT) molecules.

Experimental Chiral SFG Spectrum of Netropsin

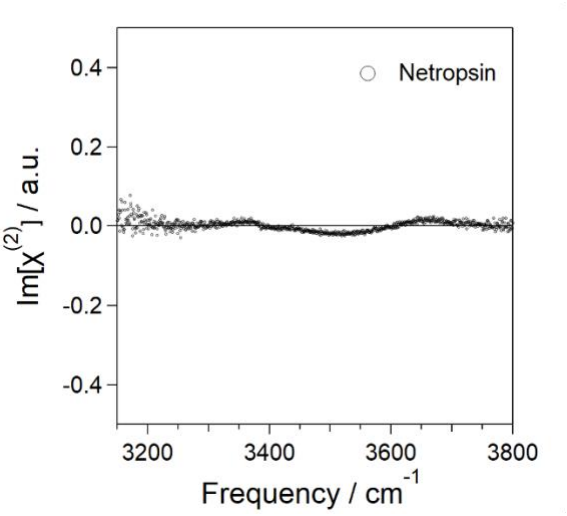

Figure S4. Chiral SFG spectrum of 50 μM aqueous solution of netropsin deposited onto the crystalline quartz substrate.

References

1. G. Ma, J. Liu, L. Fu and E. C. Yan, Probing water and biomolecules at the air–water interface with a broad bandwidth vibrational sum frequency generation spectrometer from 3800 to 900 cm− 1, *Appl. Spectrosc.*, 2009, **63**, 528-537.
2. E. A. Perets, D. Konstantinovsky, T. Santiago, P. E. Videla, M. Tremblay, L. Velarde, V. S. Batista, S. Hammes-Schiffer and E. C. Y. Yan, Beyond the "spine of hydration": Chiral SFG spectroscopy detects DNA first hydration shell and base pair structures, *J. Chem. Phys.*, 2024, **161**.
3. D. Konstantinovsky, E. A. Perets, T. Santiago, K. Olesen, Z. Wang, A. V. Soudackov, E. C. Y. Yan and S. Hammes-Schiffer, Design of an Electrostatic Frequency Map for the NH Stretch of the Protein Backbone and Application to Chiral Sum Frequency Generation Spectroscopy, *J. Phys. Chem. B*, 2023, **127**, 2418-2429.
4. E. A. Perets, D. Konstantinovsky, L. Fu, J. Chen, H.-F. Wang, S. Hammes-Schiffer and E. C. Y. Yan, Mirror-image antiparallel β-sheets organize water molecules into superstructures of opposite chirality, *Proc. Nat. Acad. Sci.*, 2020, **117**, 32902-32909.
5. N. Ji, V. Ostroverkhov, C.-Y. Chen and Y.-R. Shen, Phase-sensitive sum-frequency vibrational spectroscopy and its application to studies of interfacial alkyl chains, *J. Am. Chem. Soc.*, 2007, **129**, 10056-10057.
6. L. Fu, S.-L. Chen and H.-F. Wang, Validation of Spectra and Phase in Sub-1 cm-1 Resolution Sum-Frequency Generation Vibrational Spectroscopy through Internal Heterodyne Phase-Resolved Measurement, *J. Phys. Chem. B*, 2016, **120**, 1579-1589.
7. D. Konstantinovsky, E. A. Perets, E. C. Y. Yan and S. Hammes-Schiffer, Simulation of the Chiral Sum Frequency Generation Response of Supramolecular Structures Requires Vibrational Couplings, *J. Phys. Chem. B*, 2021, **125**, 12072-12081.
8. D. A. Case, H. M. Aktulga, K. Belfon, D. S. Cerutti, G. A. Cisneros, V. W. D. Cruzeiro, N. Forouzesh, T. J. Giese, A. W. Götz and H. Gohlke, AmberTools, *J. Chem. Inf. Model.*, 2023, **63**, 6183-6191.
9. M. L. Kopka, C. Yoon, D. Goodsell, P. Pjura and R. E. Dickerson, Binding of an antitumor drug to DNA, Netropsin and C-G-C-G-A-A-T-T-BrC-G-C-G, *J. Mol. Biol.*, 1985, **183**, 553-563.
10. X. Chen, S. N. Mitra, S. T. Rao, K. Sekar and M. Sundaralingam, A novel end-to-end binding of two netropsins to the DNA decamers d(CCCCCIIIII)2, d(CCCBr5CCIIIII)2and d(CBr5CCCCIIIII)2, *Nucleic Acids Res.*, 1998, **26**, 5464-5471.
11. W. Humphrey, A. Dalke and K. Schulten, VMD: visual molecular dynamics, *J. Mol. Graphics Modell.*, 1996, **14**, 33-38.
12. H. W. Horn, W. C. Swope, J. W. Pitera, J. D. Madura, T. J. Dick, G. L. Hura and T. Head-Gordon, Development of an improved four-site water model for biomolecular simulations: TIP4P-Ew, *J. Chem. Phys.*, 2004, **120**, 9665-9678.
13. B. Auer and J. Skinner, Dynamical effects in line shapes for coupled chromophores: Time-averaging approximation, *J. Chem. Phys.*, 2007, **127**.
14. B. Auer and J. Skinner, Vibrational sum-frequency spectroscopy of the water liquid/vapor interface, *J. Phys. Chem. B*, 2009, **113**, 4125-4130.
15. P. Pieniazek, C. Tainter and J. Skinner, Interpretation of the water surface vibrational sum-frequency spectrum, *J. Chem. Phys.*, 2011, **135**.
16. B. Auer and J. Skinner, IR and Raman spectra of liquid water: Theory and interpretation, *J. Chem. Phys.*, 2008, **128**.

17. S. Corcelli, C. Lawrence and J. Skinner, Combined electronic structure/molecular dynamics approach for ultrafast infrared spectroscopy of dilute HOD in liquid H2O and D2O, *J. Chem. Phys.*, 2004, **120**, 8107-8117.
18. D. Konstantinovsky, E. C. Y. Yan and S. Hammes-Schiffer, Characterizing interfaces by Voronoi tessellation, *J. Chem. Phys. Lett.*, 2023, **14**, 5260-5266.
19. N. Michaud-Agrawal, E. J. Denning, T. B. Woolf and O. Beckstein, MDAnalysis: a toolkit for the analysis of molecular dynamics simulations, *J. Comput. Chem.*, 2011, **32**, 2319-2327.
20. R. J. Gowers, M. Linke, J. Barnoud, T. J. E. Reddy, M. N. Melo, S. L. Seyler, J. Domanski, D. L. Dotson, S. Buchoux and I. M. Kenney, *MDAnalysis: a Python package for the rapid analysis of molecular dynamics simulations*, Report 2575-9752, Los Alamos National Laboratory (LANL), Los Alamos, NM (United States), 2019.
21. V. Ramasubramani, B. D. Dice, E. S. Harper, M. P. Spellings, J. A. Anderson and S. C. Glotzer, freud: A software suite for high throughput analysis of particle simulation data, *Comput. Phys. Commun.*, 2020, **254**, 107275.
22. C. H. Rycroft, VORO plus plus: A three-dimensional Voronoi cell library in C plus, *Chaos*, 2009, **19**.